Scottish Universities Environmental Research Centre

Luminescence dating of sediments from two sites near Anuradhapura, Sri Lanka

May 2009

A.J. Cresswell, D.C.W. Sanderson
Scottish Universities Environmental Research Centre,
East Kilbride, G75 0QF
I.A. Simpson
School of Biological & Environmental Sciences,
University of Stirling, Stirling, FK9 4LA

East Kilbride Glasgow G75 0QF Telephone: 01355 223332 Fax: 01355 229898

University of Glasgow

Summary

Previous Optical Stimulated Luminescence (OSL) investigations of irrigation features and archaeological sites in the hinterland around Anuradhapura, Sri Lanka, had observed highly heterogeneous dose distributions and apparent ages older than expected for bunds and similar constructions. These observations are consistent with utilising older sedimentary materials, which did not have their luminescence signals reset during construction.

The work reported here consists of OSL measurements from two sites in the Anuradhapura region. The first is a modern bund, sampled to examine the degree of heterogeneity of the dose distributions from a control structure. Two samples were taken from within this bund, one near the top and the other just above the land surface the bund was built upon. These show dose distributions that are highly heterogeneous with apparent ages in excess of 1500 years. The third sample from this site is from the truncated land surface beneath the bund, and gives a luminescence age of 150 ± 40 years with just one much older aliquot.

The second site in this work is an abandoned red-earth platform site, covered by an extensive layer of cultural deposits. A sample from the overlying deposits just above the constructed platform gives a luminescence age of 540 ± 70 years, with a homogenous dose distribution. A sample from near the top of the constructed platform gives a heterogeneous dose distribution and apparent ages up to 4000 years.

The results support the inferences from earlier sampling, providing clear confirmation that platform sites contain unbleached, re-deposited sediments, with significant residual OSL ages. The OSL results from the underlying land surfaces, and from slowly accumulated abandonment layers, appear to be consistent with external age control where available and thus are to be preferred as targets for OSL dating in such geo-archaeological investigations.

Contents

1. Introduction

This report is concerned with optically stimulated luminescence (OSL) investigations of sediment samples recovered from locations in the Anuradhapura Hinterland, Sri Lanka (80°22' to 80°51' E, 8°08' to 8°24' N). Samples were taken by Ian Simpson in August 2008. These are additional samples following on from earlier OSL investigations reported in Burbidge *et.al.* 2008 where it was noted that some sites tended to contain material with heterogeneous dose distributions and apparent ages older than underlying land surfaces.

Samples were collected from two sites. One is a modern bund to allow investigation of the magnitudes of heterogeneous dose distributions and excess ages from a contemporary system. The second is an additional abandoned construction platform with an archaeological context under investigation.

2. Sampling

Sampling was undertaken in the Anuradhapura Hinterland in August 2008. Samples for luminescence analysis were taken, as before, by driving copper tubes into the cleaned face of excavated sections, then sealing the tubes with foil and tape upon their extraction. The sampling holes were enlarged for field gamma spectrometry, and bulk sediments collected near the location of each tube. Three samples were taken from a modern bund; one from the truncated land surface beneath the bund and two from the bund, and a further two samples from an ancient platform, one sample from a constructed layer and another from the accumulated cultural deposits overlying the platform.

Sampling details, including the names assigned to each tube and bulk sample in the field, and the laboratory (SUTL) numbers assigned to each upon arrival at the SUERC luminescence dating laboratories, are summarised in Table 2.1. Section diagrams for the two sites are included in the Appendix.

Table 2.1. Sample locations, descriptions, and SUERC laboratory numbers

SUERC	Sample Number Field	Coordinates E	N	Depth[a] (cm)	Description
SUTL2270	Modern Bund OSL1	80°30.899	8°19.970	170	Reddish-brown sandy clay loam, very stony
SUTL2271	Modern Bund OSL2			193	Light brownish gray sandy loam, truncated land surface beneath bund
SUTL2272	Modern Bund OSL3			49	Dark yellowish brown sandy clay, buried bund land surface
SUTL2273	Trench 2A, site B-62 OSL1	80°23.587	8°25.304	56	Dark reddish-brown sandy clay loam, cultural deposits overlaying constructed platform
SUTL2274	Trench 2A, site B-62 OSL2			65	Dark reddish-brown very coarse sandy clay, near top of constructed platform

[a] estimated from section diagrams

3. Methods

3.1. Sample preparation

All sample handling and preparation was conducted under safelight conditions in the SUERC luminescence dating laboratories.

Water content was determined from the bulk samples collected near the OSL sampling locations. The entire bulk sample was weighed, then topped up with water until saturated and reweighed. The sample was then dried in an oven for at least 24h before being reweighed. This analysis yields the water content of the bulk material at time of sampling, and the maximum limit of the water content assuming saturation. An assumed average water content for the material is then taken as the mean of these values.

100 g of the dried bulk material was weighed into HDPE pots for high-resolution gamma spectrometry (HRGS) measurement. The pots were sealed with epoxy resin and left for at least 4 weeks prior to measurement to allow equilibration of ^{222}Rn daughters. A further 20 g of the dried bulk material was used for thick source beta counting (TSBC) measurements.

Approximately 10-15 g of material from the core of each sample tube was processed for luminescence measurements. With the object of separating sand-sized quartz grains from the bulk sediment, luminescence sub-samples were wet sieved to obtain 150-250 μm grains, which were treated with 1 M HCl for 10 minutes to dissolve carbonates, and then treated with 40% Hydrofluoric acid (HF) for 40 minutes, to dissolve less chemically resistant minerals and to etch the outer part of the quartz grains. The HF etched material was then treated with 1 M HCl for 10 minutes to dissolve any precipitated fluorides. This etched material was then centrifuged in sodium polytungstate with a density of ~2.8 g cm^{-3} to separate quartz from other heavy minerals present. The light, quartz, fraction was then dried at 50°C, and dispensed onto the central part of 1 cm diameter, 0.25 mm thick stainless steel disks, using silicone oil for adhesion. 16 disks were made per sample.

20g of dried material from each sampling tube was also used for TSBC measurements, as a cross-check that the dosimetry data from the bulk sample was representative of the sample used for OSL.

3.2. Measurements and determinations

3.2.1. Dose rate measurements and determinations

Dose rates were measured in the laboratory using High Resolution Gamma Spectrometry (HRGS) and Thick Source Beta Counting (TSBC). In-situ gamma spectra were measured using a Field Gamma Spectrometer (FGS) at the time of sampling. Full sets of dose rate determinations were made for all samples.

FGS measurements were made using an Ortec DigiBASE spectrometer pack with a 2"x 2" NaI probe. Prior to 2006 fieldwork, measurements were made using this

system on the doped concrete reference pads at SUERC in order to provide cross-reference to dose-rate conversion factors established by Sanderson (1986), based on comparisons with TL dosimetry in doped blocks then at the Oxford and Risø luminescence laboratories. The spectra were calibrated to the 1461 keV peak from ^{40}K and the 2614.5 keV peak from ^{208}Tl, then dose rates were determined from integral counts >450 keV, >1350 keV. Using this approach yielded dose rates from the pads that were on average within 2% and 5% of those expected for the >450 keV and >1350 keV integrals. Field spectra were each measured for ~1 hr in holes cut around the luminescence sampling positions using an over-tube, and calibrated to the 1461 keV peak from ^{40}K and the 2614.5 keV peak from ^{208}Tl before calculation of dose rates.

HRGS measurements were performed using a 50% relative efficiency "n" type hyper-pure Ge detector (EG&G Ortec Gamma-X) operated in a low background lead shield with a copper liner. Gamma ray spectra were recorded over the 30 keV to 3 MeV range from each sample, interleaved with background measurements and measurements from Shap Granite in the same geometries. Counting times of 80 ks per sample were used. The spectra were analysed to determine count rates from the major line emissions from ^{40}K (1461 keV), and from selected nuclides in the U decay series (^{234}Th, ^{226}Ra + ^{235}U, ^{214}Pb, ^{214}Bi and ^{210}Pb) and the Th decay series (^{228}Ac, ^{212}Pb, ^{208}Tl) and their statistical counting uncertainties. Net rates and activity concentrations for each of these nuclides were determined relative to Shap Granite by weighted combination of the individual lines for each nuclide. The internal consistency of nuclide specific estimates for U and Th decay series nuclides was assessed relative to measurement precision, and weighted combinations used to estimate mean activity concentrations (in Bq kg^{-1}) and elemental concentrations (% K and ppm U, Th) for the parent activity. These data were used to determine infinite matrix dose rates for alpha, beta and gamma radiation.

Beta dose rates were also measured directly using the SUERC TSBC system (Sanderson, 1988). Sample count rates were determined with six replicate 600 s counts for each sample, bracketed by background measurements and sensitivity determinations using the SUERC Shap Granite secondary reference material. Infinite-matrix dose rates were calculated by scaling the net count rates of samples and reference material to the working beta dose rate of the Shap Granite (6.25±0.03 mGy a^{-1}). The estimated errors combine counting statistics, observed variance and the uncertainty on the reference value.

"Field" and "saturated" values of water content (section 3.1) were calculated as fractions of dry sediment mass. An assumed value for the average water content during burial was calculated as the average of the field and saturated water contents. The dose rate estimates were used in combination with the assumed burial water contents, to determine the overall effective dose rates for age estimation.

The cosmic dose rate was estimated as follows. The latitude, altitude and (sediment) depth dependencies of cosmic radiation, relevant to luminescence dating, are described by Prescott and Stephan (1982) and Prescott and Hutton (1988). In the present study, the latitude of each sample was approximated to the nearest degree, and altitude was approximated as 0.1 km for all. Surface cosmic dose rate was estimated

using Prescott and Stephan (1982), Eqn. 1, with latitude dependent parameters read from Fig. 2. A representative value for the average burial depth of each sample since the luminescence signal was last zeroed, was estimated from depth at the time of sampling, geomorphological context, and approximate luminescence age. Depth was converted to mass-depth assuming sediment bulk density to be 1.6 g/cm^3, and a fit to the dose rate vs. depth data of Prescott and Hutton (1988) was used to calculate the cosmic dose rate at that depth. Uncertainties were calculated as: 5% plus the difference between cosmic dose rate at the depth of sampling, and that at the estimated average burial depth.

3.2.2. Luminescence measurements

All measurements were conducted using a Risø DA-15 automatic reader equipped with a ^{90}Sr/^{90}Y β-source for irradiation, blue LEDs emitting around 470 nm and infrared (laser) diodes emitting around 830 nm for optical stimulation, and a U340 detection filter pack to detect in the region 270-380 nm, while cutting out stimulating light (Bøtter-Jensen *et al.*, 2000).

The discs of quartz grains from the tube samples were subjected to a single aliquot regeneration (SAR) sequence (cf Murray and Wintle, 2000). According to this procedure, the OSL signal level from an individual disc is calibrated to provide an absorbed dose estimate (the equivalent dose) using an interpolated dose-response curve, constructed by regenerating OSL signals by beta irradiation in the laboratory. Sensitivity changes which may occur as a result of readout, irradiation and preheating (to remove unstable radiation-induced signals) are monitored using small test doses after each regenerative dose. Each measurement is standardised to the test dose response determined immediately after its readout, to compensate for observed changes in sensitivity during the laboratory measurement sequence. For the purposes of interpolation, the regenerative doses are chosen to encompass the likely value of the equivalent (natural) dose. A repeat dose point is included to check the ability of the SAR procedure to correct for laboratory-induced sensitivity changes (the "recycling test"), a zero dose point is included late in the sequence to check for thermally induced charge transfer during the irradiation and preheating cycle (the "zero cycle"), and an IR response check is included to assess the magnitude of non-quartz signals.

In the present study 16 discs per sample were measured using 4 discs each at 4 different preheats (Table 3.1). A slowly decaying component in the OSL signals appeared to come from traps producing TL in the range 200-280°C: differential effects such as variations in De vs. time were reduced by matching the test and regenerative preheats. Regenerative doses of 0 to 15 Gy were applied to all samples (plus repeats etc.: cycles 1 to 9, Table 3.1). Before the samples were removed from the Riso reader, the data was examined briefly to determine whether the equivalent dose exceeded 15Gy, in those cases where this seemed possible (SUTL2270 and 2272) additional 18Gy and 21Gy regenerative doses were applied.

Table 3.1. Quartz Single Aliquot Regenerative Sequence

Aliquots	Operation	Details	Cycle: 1 Natural	2	3	4	5	6	7 Zero	8 Recycling	9 IR Response
				Linear-spaced low doses							
1-16	Regenerative Dose	"X" Gy ^{90}Sr/^{90}Y	no	3	6	9	12	15	0	3	3
1-4	Preheat	200°C for 30s	yes	yes	yes	yes	yes	yes	yes	yes	yes
4-8	Preheat	220°C for 30s	yes	yes	yes	yes	yes	yes	yes	yes	yes
9-12	Preheat	240°C for 30s	yes	yes	yes	yes	yes	yes	yes	yes	yes
13-16	Preheat	260°C for 30s	yes	yes	yes	yes	yes	yes	yes	yes	yes
1-16	Measurement	IRSL 120s at 50°C	no	no	no	no	no	no	no	no	yes
1-16	Measurement	OSL 60s at 125°C	yes	yes	yes	yes	yes	yes	yes	yes	yes
1-16	Test Dose	"X" Gy ^{90}Sr/^{90}Y	1	1	1	1	1	1	1	1	1
1-16	Test Preheat	160°C for 30s	yes	yes	yes	yes	yes	yes	yes	yes	yes
1-16	Test Measurement	OSL 60s at 125°C	yes	yes	yes	yes	yes	yes	yes	yes	yes

4. Results

4.1. Dose rates

HGRS results are shown in Table 4.1, both as activity concentrations (i.e. disintegrations per second per kilogram) and as equivalent parent element concentrations (in % and ppm), based in the case of U and Th on combining nuclide specific data assuming decay series equilibrium.

Infinite matrix alpha, beta and gamma dose rates from HGRS are listed in Table 4.2, with in-situ gamma dose rates from FGS, infinite matrix beta dose rates from TSBC, and the ratio of beta dose rates from TSBC/HGRS. Comparison of the TSBC dose rates for material from the sample tubes and the bulk samples indicates that the bulk material appears to be representative of the dose rate for the sampling tubes. For SUTL2270-2272, the TSBC and HRGS beta dose rates agree very well. For SUTL2273 and SUTL2274, the TSBC beta dose rate is larger than that from the HRGS. It has been noted for these samples, but not for the three in good agreement, that the HRGS data show enhancement in ^{234}Th relative to the other isotopes further down the ^{238}U decay chain which would explain the higher TSBC beta dose rate compared to the HRGS. The ^{234}Th enhancement in the samples from the B-62 site is potentially indicative of either systemic uranium re-deposition in the vicinity of the sample (which would be accompanied by U series disequilibrium to ^{230}Th, or leaching of ^{226}Ra. Alpha spectrometry or mass spectrometry measurements of the state of U series disequilibrium would be needed to distinguish between these two scenarios, and produce a time dependent dose rate model for the samples

Effective dose rates to the HF etched 200 μm quartz grains used for equivalent dose determination in the present study are listed in Table 4.3, with water content measurements and the assumed values used for calculation of effective dose rate. Cosmic dose rates are as calculated (section 3.2.1), gamma and beta dose rates are corrected for water content.

The ratio of gamma dose rates from FGS and HGRS, after adjustment for assumed levels of water content, ranged from 0.8 to 1.30.

To accommodate the range of likely sample conditions during burial, the weighted means of the TSBC and HGRS values, and the FGS and HRGS values, were used for the calculation of effective beta and gamma dose rates to the samples, with "external error" values (e.g. Burbidge *et al.*, 2006).

Table 4.1. Activity and equivalent concentrations of K, U and Th, determined by HRGS

SUTL No.	Activity Concentration (Bq kg⁻¹)[a]			Equivalent Concentration[b]			Th/U
	^{40}K	^{214}Bi	^{208}Tl	K (%)	U (ppm)	Th (ppm)	
2270	598 ± 10	31.4 ± 0.8	41.8 ± 0.4	1.93 ± 0.03	2.54 ± 0.07	10.31 ± 0.10	4.06 ± 0.12
2271	665 ± 11	32.7 ± 0.9	39.1 ± 0.4	2.15 ± 0.04	2.64 ± 0.07	9.64 ± 0.09	3.65 ± 0.10
2272	503 ± 9	25.4 ± 0.6	32.5 ± 0.3	1.63 ± 0.03	2.06 ± 0.05	8.01 ± 0.08	3.89 ± 0.10
2273	214 ± 6	7.4 ± 0.2	11.7 ± 0.2	0.69 ± 0.02	0.60 ± 0.02	2.88 ± 0.05	4.80 ± 0.18
2274	81 ± 5	3.7 ± 0.2	6.5 ± 0.2	0.26 ± 0.02	0.30 ± 0.01	1.59 ± 0.04	5.30 ± 0.22

[a] Shap granite reference, working values based on HRGS relative to CANMET and NBL standards by Sanderson (1986).
[b] Activity and equivalent concentrations for U, Th and K determined by HRGS. Conversion factors based on OECD (1994): 40K: 309.3 Bq/kg/%K, 238U: 12.35 Bq/kg/ppmU, 232Th: 4.057 Bq/kg/ppmTh.

Table 4.2. Insitu gamma dose rate measured using FGS, and infinite matrix dose rates determined by HRGS and TSBC in the laboratory.

SUTL No.	FGS, In-situ gamma (mGy a⁻¹)	HRGS, Dry (mGy a⁻¹)			TSBC, Dry (mGy a⁻¹)		TSBC/ HRGS
		Alpha	Beta	Gamma	Bulk	Sample	
2270	0.868 ± 0.043	14.7 ± 0.2	2.27 ± 0.03	1.288 ± 0.012	2.45 ± 0.06	2.56 ± 0.06	1.08 ± 0.03
2271	0.834 ± 0.042	14.5 ± 0.2	2.45 ± 0.03	1.317 ± 0.013	2.64 ± 0.06	2.56 ± 0.06	1.08 ± 0.03
2272	0.761 ± 0.038	11.6 ± 0.2	1.88 ± 0.03	1.040 ± 0.010	2.02 ± 0.05	2.10 ± 0.06	1.07 ± 0.03
2273	0.286 ± 0.014	3.79 ± 0.06	0.75 ± 0.02	0.384 ± 0.006	1.25 ± 0.05	1.31 ± 0.05	1.67 ± 0.08
2274	0.195 ± 0.010	2.01 ± 0.05	0.31 ± 0.01	0.180 ± 0.005	0.55 ± 0.04	0.48 ± 0.04	1.77 ± 0.14

Table 4.3. Water contents and effective dose rates

| SUTL No.	Water Content (%)			Gamma (mGy a⁻¹)		Effective Dose Rate (mGy a⁻¹)		
	Field	Sat.	Assumed	FGS	HRGS	Beta	Gamma	Cosmic
2270	14.3	35.5	23 ± 3	0.868 ± 0.043	1.03 ± 0.03	1.70 ± 0.08	0.947 ± 0.026	0.19 ± 0.08
2271	14.0	29.3	20 ± 3	0.834 ± 0.042	1.08 ± 0.03	1.84 ± 0.09	0.956 ± 0.026	0.19 ± 0.09
2272	4.2	17.8	10 ± 3	0.761 ± 0.038	0.94 ± 0.03	1.60 ± 0.08	0.849 ± 0.024	0.24 ± 0.04
2273	4.6	25.3	14 ± 3	0.286 ± 0.014	0.332 ± 0.011	0.85 ± 0.06	0.309 ± 0.009	0.23 ± 0.04
2274	5.1	30.3	16 ± 3	0.195 ± 0.010	0.152 ± 0.006	0.33 ± 0.04	0.173 ± 0.006	0.23 ± 0.05

4.2. Single aliquot equivalent dose determinations

Sample averaged values relating to the aliquots and measurements used for equivalent dose determination are listed in Table 4.4.

For equivalent dose determination, data from single aliquot regenerative dose measurements were analysed using the Risø TL/OSL Viewer programme to export integrated summary files that were analysed in MS Excel and SigmaPlot. Dose response curves for each of the four pre-heating temperature groups and the combined data were determined using a fit to a saturating exponential function in the first instance. Where the exponential fit was poorly constrained a linear fit was used. Values of De were determined for each group of disks and each individual disk. Figure 4.1 shows the De values determined for each disk. It is clear that, with the exception of a few outliers and low precision values, SUTL2271 and SUTL2273 show homogenous behaviour consistent with material with a well defined age. For the other samples, there is considerable heterogeneity between disks consistent with mixed materials of different OSL ages. From these stratigraphic contexts, and the depositional systems associated with built platforms, this is unsurprising and suggests that the OSL dates should be treated as "apparent ages" rather than physical time intervals. The possibility that additional studies of single grains or small aliquots could help is discussed briefly in section 5.

Arithmetic mean De values are listed for each sample in Table 4.4, with the estimated uncertainty on the mean value (standard deviation divided by the square root of the number of disks), and the standard deviation of the dataset. Weighted means are given that reduce the influence of low precision data points. Robust mean De data generated using Huber's estimate 2 (H15) using the Royal Society of Chemistry robust statistics toolkit for MS Excel (Ellison 2002).

Figure 4.1: De values determined for each of 16 disks for the five OSL samples
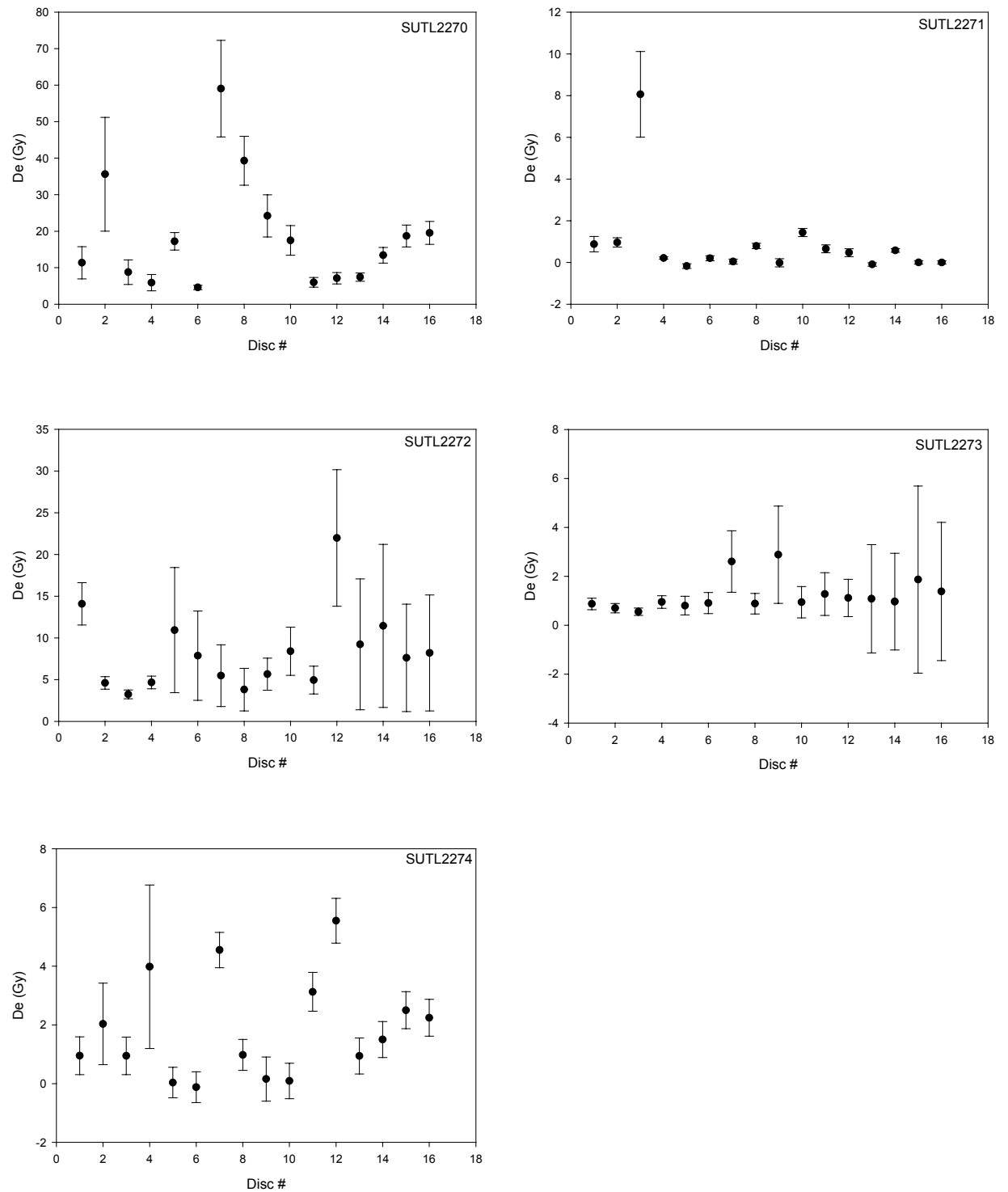
Table 4.4. Equivalent dose determination: samples and results

SUTL No.	Sensitivity (cps Gy⁻¹)	Sensitivity change (%)	Recycling ratio	Post IRSL Ratio (%)	Equivalent Dose (Gy)			
					Linear Mean	Weighted Mean	Robust Mean	Best Estimate
2270	1904 ± 214	2.5 ± 22.6	1.04 ± 0.03	2.5 ± 0.1	18.47 ± 3.73	7.20 ± 0.42	16.20 ± 2.81	
2271	922 ± 39	29.1 ± 9.8	1.04 ± 0.06	1.1 ± 0.2	0.87 ± 0.49	0.21 ± 0.03	0.43 ± 0.13	0.43 ± 0.13
2272	15911 ± 1524	3.6 ± 19.5	1.09 ± 0.01	11.7 ± 0.1	8.26 ± 1.19	4.39 ± 0.35	7.60 ± 0.90	
2273	8750 ± 960	27.7 ± 25.3	1.18 ± 0.02	5.8 ± 0.1	1.24 ± 0.17	0.75 ± 0.09	1.09 ± 0.10	0.75 ± 0.09
2274	1595 ± 85	66.0 ± 14.4	1.54 ± 0.09	-0.6 ± 0.6	1.84 ± 0.43	1.51 ± 0.16	1.74 ± 0.43	

11

4.3. Age estimates

Listed in Table 4.5 are the sums of the effective beta, gamma and cosmic dose rates and the equivalent dose estimates. Age values were calculated as equivalent dose divided by dose rate, and converted to calendar dates.

Table 4.5. Dose rates, equivalent doses, ages and calendar dates

Sample Number		Total Dose Rate (mGy a^{-1})	Equivalent Dose (Gy)	Apparent age (ka)	Error (%)	Calendar date
SUERC	Field					
SUTL2270	Modern Bund OSL1	2.83 ± 0.12	5 - 20	1.8 - 7.1		
SUTL2271	Modern Bund OSL2	2.99 ± 0.13	0.43 ± 0.13	0.15 ± 0.04	30.3	1865 ± 45 AD
SUTL2272	Modern Bund OSL3	2.69 ± 0.10	4 - 10	1.5 - 3.7		
SUTL2273	B-62 Trench 2A OSL1	1.39 ± 0.07	0.75 ± 0.09	0.54 ± 0.07	12.7	1465 ± 70 AD
SUTL2274	B-62 Trench 2A OSL2	0.74 ± 0.07	0 - 3	0 - 4.1		

5. Discussion

Samples were analysed from two sites.

The first of these was a modern bund, examined to investigate the extent to which older sedimentary material within the bund construction is reflected in the OSL data. For this site, the sample collected from the truncated land surface beneath the bund has a well defined age of 150 ± 40 years, consistent with a later bund construction in the modern period. The samples collected from within the bund show considerable heterogeneity in the De determination by OSL, with average apparent ages significantly older than the underlying land surface. This is consistent with the bund construction utilising sediments from much older contexts that have not been bleached by daylight during the construction of the bund.

The second site was an abandoned platform, overlain by cultural deposits. The sample from the platform showed a heterogeneous De distribution, similar to that observed in the modern bund. The sample from the overlaying cultural deposits was significantly more homogenous, with an age of 540 ± 70 years. The data is consistent with a structure that was abandoned at least 550 years ago, and subsequently buried by material that was laid down with little or no residual luminescence signal.

The results support the inferences from earlier sampling within this project, and provide a clear confirmation that the structures themselves contain unbleached, re-deposited sediments, with significant residual OSL ages. The data verify the effectiveness of dose distributional analysis and the SAR method in identifying such material, even using aliquots with several hundred quartz grains. This should add to the confidence in the explanations put forward for the excess OSL ages determined from such structures elsewhere in the project. By contrast the OSL results from the underlying land surfaces, and from slowly accumulated abandonment layers appear to be consistent with external age control where available and thus are to be preferred as targets for OSL dating in such geo-archaeological investigations. While there is scope for further research to investigate whether small aliquot analysis or single grain analysis (eg Olley *et al* 1998,1999, Spencer *et al* 2003, Duller *et al* 2000) could help to address the complex mixing and residuals within such material, it is by no means clear that such work would lead to unambiguous age assessment of the constructional age of such features. Similar examples of re-deposited layers in archaeological features have been demonstrated in studies of ancient canal sediments (Sanderson *et al* 2003, 2007), in Palaeolithic sequences (Burbidge *et al*, 2008) and in Neolithic ditch fills (Sanderson *et al* 2009). In all of these cases luminescence profiling, using small sequence of diagnostic samples analysed in the laboratory, or using portable OSL equipment, have been effective in identifying luminescence inversions or discontinuities associated with re-deposited layers, and thus helping to understand the depositional process in support of sediment dating. Such procedures would be useful in future work in this area as well.

References

Bøtter-Jensen, L., Bulur, E., Duller, G.A.T., and Murray, A.S. (2000). Advances in luminescence instrument systems. *Radiation Measurements* 32, 523-528.

Burbidge, C.I., Sanderson, D.C.W., Simpson, I.A, Adderley, W.P. 2007. Luminescence dating of sediments from ancient irrigation features, and associated with occupation of the hinterland around Anuradhapura, Sri Lanka. Glasgow, SUERC, University of Glasgow: pp145.

Burbidge, C.I., Sanderson, D.C.W., Fülöp, R. (2008). *Luminescence dating of ditch and pitfills from Newry Ring Fort, Northern Ireland.* SUERC, East Kilbride, 91pp.

Duller, G.A.T, Bøtter-Jensen, L., Murray, A.S. (2000). Optical dating of single sand-sized grains of quartz: sources of variability. *Radiation Measurements* 32, 453-457.

Ellison, S (2002). Royal Society of Chemistry AMC Technical Brief no. 6. www.rsc.org/lap/rsccom/amc/amc_index.htm

Mejdahl, V. (1979). Thermoluminescence dating: Beta-dose attenuation in quartz grains. *Archaeometry* 21, 61-72.

Murray, A.S., and Wintle, A.G. (2000). Luminescence dating of quartz using an improved single-aliquot regenerative-dose protocol. *Radiation Measurements* 32, 57-73.

Olley, J., Caitcheon, G., Murray, A.S. (1998). The distribution of apparent dose as determined by optically stimulated luminescence in small aliquots of fluvial quartz: implications for dating young sediments. *Quaternary Science Reviews (Quaternary Geochronology)* 17, 1033-1040.

Olley, J., Caitcheon, G., Roberts, R.G. (1999). The origin of dose distributions in fluvial sediments, and the prospect of dating single grains from fluvial sediments using optically stimulated luminescence. *Radiation Measurements* 30, 207-217.

Prescott, J.R., and Hutton, J.T. (1988). Cosmic-Ray and Gamma-Ray Dosimetry For Tl and Electron-Spin- Resonance. *Nuclear Tracks and Radiation Measurements* 14, 223-227.

Prescott, J.R., and Stephan, L.G. (1982). The contribution of cosmic radiation to the environmental dose for thermoluminescent dating. Latitude, altitude and depth dependencies. *PACT* 6, 17-25.

Sanderson, D.C.W. (1986). Luminescence Laboratory Internal Report. SURRC.

Sanderson, D.C.W. (1988). Thick Source Beta-Counting (TSBC) - a Rapid Method for Measuring Beta-Dose-Rates. *Nuclear Tracks and Radiation Measurements* 14, 203-207.

Sanderson, D.C.W., Bishop, P., Stark, M.T., Spencer, J.Q. (2003). Luminescence dating of anthropologically reset sediments from Angkor Borei, Mekong Delta, Cambodia. *Quaternary Science Reviews*, 22(10-13), 1111-1122.

Sanderson, D.C.W. *et.al.* (2007). Luminescence dating of canal sediments from Angkor Borei, Mekong Delta, Southern Cambodia. *Quaternary Geochronology*, 2(1-4), 322-329.

Sanderson, D.C.W, Murphy, S. (2009). Using simple portable OSL measurements and laboratory characterization to help understand complex and heterogeneous sediment sequences for luminescence dating. *Quaternary Geochronology*, doi:10.1016/j.quageo.2009.02.001

Spencer, J.Q., Sanderson, D.C.W., Deckers, K., Sommerville, A.A. (2003). Assessing mixed dose distributions in young sediments identified using small aliquots and a simple two step SAR procedure: the F-statistic as a diagnostic tools. *Radiation Measurements* 37, 425-431.

Appendix: Section diagrams

Trench 2A, site B-62
Anuradhapura Hinterland

8° 25.304 N
80° 23.587 E

1. 5YR 3/3 dark reddish brown sandy clay loam.
2. 5YR 2.5/2 dark reddish brown sandy clay loam.
3. 2.5YR 2.5/4 dark reddish brown very coarse sandy clay.
4. 7.5YR brown very coarse sandy clay loam.
5. 5YR 3/4 dark reddish brown very coarse sandy clay loam.
6. 7.5YR 4/3 brown sandy loam.
7. 2.5YR 2.5/4 dark reddish brown very coarse sandy clay loam.
8. 5YR 4/5 reddish brown coarse sandy clay loam.

Legend:
- OSL sample
- Bulk sample
- Kubiena tin
- Stone
- pottery
- Bedrock

0 cm 20

16

OSL 3

K3

K1

K2
OSL 1

OSL 2
K4

unexcavated

① 10YR 5/6 yellowish brown
sandy loam.

② 10YR 3/6 dark yellowish brown
gravelly sandy clay, 2% manganese nodules.

③ 10YR 3/4 dark yellowish brown
sandy clay, 2% manganese nodules.

④ 2.5YR 3/6 dark red
sandy clay, stony, 7% manganese nodules.

⑤ 10YR 5/4 yellowish brown
sandy loam, very stony, 2% manganese nodules.

⑥ 10YR 5/3 brown to 7.5YR 4/3 brown
sandy clay, stony, 5% manganese nodules
5YR 4/6 yellowish red coating on very fine
root channels.

⑦ 10YR 3/6 dark yellowish brown
sandy clay, 5% manganese nodules
sticks buried within unit.

⑧ 2.5YR 3/4 dark reddish brown
sandy clay loam, very stony
2% manganese nodules
branches buried within this unit.

⑨ 2.5YR 6/2 light brownish gray
sandy loam, 2% manganese nodules
faint mottles 7.5YR 6/8, reddish yellow.

⑩ 10YR 5/4 yellowish brown loamy sand
40% distinct mottles, 7.5YR 5/8 strong brown.

⑪ 10YR 5/4 yellowish brown loamy sand.

⑫ 2.5YR 4/6 red gravelly sandy clay loam.

⑬ 10YR 5/4 yellowish brown sandy clay loam
30% distinct mottles,
7.5YR 5/8 strong brown,
1% manganese nodules.

•   OSL sample
o   Bulk sample
▢   Kubiena tin

0   cm   20

17